Title
Status Report to USNDC

Author
Lawrence Berkeley National Laboratory

Publication Date
1973-04-01

UCID - 16258 + Addendum
c.1

LAWRENCE LIVERMORE LABORATORY
University of California/Livermore, California

April 25, 1973

TO: USNDC Members and Contributors

FROM: John D. Anderson
John C. Browne

SUBJECT: Status Report to USNDC*

*Work performed under the auspices of the United States Atomic Energy Commission.

Prepared for U. S. Atomic Energy Commission under contract no. W-7405-Eng-48

Addition to LLL Status Report to USNDC (UCID-16258)

Atlas of Photoneutron Cross Sections Obtained with Monoenergetic Photons (B. L. Berman)

A compilation, in a uniform format and current as of early 1973, of photoneutron cross-section data obtained with monoenergetic photons from positron annihilation in flight has been issued as UCRL-74622. This atlas was distributed at the International Conference on Photonuclear Reactions and Applications in March. The USNDC has, of course, expressed its great desire that such a compilation be made available for a variety of applications purposes.

Over the years, a considerable body of data on photoneutron cross sections obtained with monoenergetic photons from the annihilation in flight of fast positrons has been acquired at the Livermore, Saclay, and General Atomic Laboratories. The data on 65 nuclei studied with annihilation photons (49 from Livermore measurements, 25 from Saclay, and two from General Atomic) are gathered together here and presented in a uniform format, in order to serve as a nucleus for a more complete compilation and evaluation (which would include data obtained with continuous bremsstrahlung radiation sources as well). The photonuclear group at the National Bureau of Standards is undertaking such a comprehensive compilation and evaluation, and the data in this atlas will be a major part of it. Meanwhile, these data are available in both graphical and digital form. It is hoped that this service to the physics community will be utilized both for purposes of theoretical analysis and for those associated with applications to other scientific disciplines and technologies.

No attempt was made here to evaluate the data; i.e., to choose between two sets of data for the same nucleus measured at different laboratories, or to compromise between them by presenting a set of recommended intermediate values. It should be noted, however, that the overall agreement and consistency between measurements made at the three laboratories is very good indeed, especially when viewed in the light of the enormous discrepancies between laboratories frequently obtained in the past for bremsstrahlung-induced photonuclear measurements.

LAWRENCE LIVERMORE LABORATORY

A. NEUTRON PHYSICS

1. ^{235}U Fission Cross-Section Measurements (J. B. Czirr and G. S. Sidhu) Relevant to Requests 388, 389, 390 and 391.

Cross-section measurements are currently underway at the LLL Linac on the ratio of the ^{235}U fission to (n,p) scattering cross section from 2 to 20 MeV.

The fission data are obtained from twelve planar 0.1 mg/cm^2 foils placed in a cylindrical fission chamber. This chamber is rotated relative to the neutron beam in order to compensate for changes in the fission fragment angular distribution with incident neutron energy.

The neutron flux measurement is obtained from a recoil-proton telescope used in ring geometry with a ^{7}Li-glass scintillator as the proton detector. A 1 mg/cm^2 polyethylene radiator foil is replaced by a deposited carbon foil for background measurements.

Cross-section measurements from thermal to 2 MeV are planned following the completion of the above experiments. The accurate normalization of the high energy data to the well-known thermal values will await these latter results.

2. Fission $\bar{\nu}$ Measurements (R. E. Howe, T. W. Phillips and C. D. Bowman*) Relevant to Requests 395 and 452.

We are currently performing measurements of $\bar{\nu}$ for neutron-induced fission of ^{235}U in the energy range 0.5 to 100 eV. Fast, spectrally-independent detection of the prompt fission neutrons is achieved with the system previously described.**

Recent work has lowered experimental background rates and electronic deadtimes thus greatly reducing the magnitude of corrections applied to the data.

We are hoping to present our results at the IAEA Third Symposium on the Physics and Chemistry of Fission, August 13-17, 1973.

Future plans include completion of $\bar{\nu}$ measurements for ^{235}U from thermal energy up to 15 MeV. We also plan to evaluate $\bar{\nu}$ for ^{239}Pu neutron-induced fission over a similar energy range.

---

* National Bureau of Standards, Washington, D.C.

** USNDC Report, dated 10 November 1971, UCID-15937.

3. Isomeric Fission in ^{243}Pu (J. C. Browne and C. D. Bowman*)
Relevant to Request 483.

Analysis of the results from an investigation of γ-decay emission from subthreshold fission groups** to the ground state in the second well for ^{243}Pu indicates the possibility of the existence of two fission isomers for this nucleus, one being the 33-ns isomer already observed and another being much longer-lived (∿100μs). If this is the case, the 33-ns isomer is consistent with being a two-quasiparticle state at an excitation energy of approximately 1.2 MeV above the ground state in the second well (whose excitation energy was previously measured to be 1.86 MeV above the equilibrium ground state). This work has been submitted for presentation at the Third Symposium on the Physics and Chemistry of Fission at Rochester, August 13-17, 1973.

4. Thermal-Neutron Fission Cross Sections of ^{251}Cf and ^{255}Fm
(R. C. Ragaini, E. K. Hulet, R. W. Lougheed and J. F. Wild)

The thermal-neutron fission cross sections of ^{251}Cf and ^{255}Fm have been measured by comparison of fission rates with a ^{233}U reference standard. The values obtained are 4800 ± 250 barns for ^{251}Cf and 3400 ± 170 barns for ^{255}Fm. An initially pure sample of 20.3-h ^{255}Fm was fission counted alternately with a ^{233}U standard in the thermal column of the LPTR during its decay to 900-y ^{251}Cf. The atoms of ^{255}Fm-^{251}Cf and ^{233}U present on the thin targets were accurately determined by α-pulse analysis. A value of 531 barns was used for the fission cross section of ^{233}U in calculating the cross sections of ^{251}Cf and ^{255}Fm.

5. Decay of ^{248}Cf (E. K. Hulet and J. F. Wild)

The total half-life of ^{248}Cf has been determined to be 333.5 ± 2.8 d by long-term alpha and fission counting in ionization chambers. In addition, the alpha-to-spontaneous fission disintegration ratio was determined to be 35000 ± 3000, resulting in a SF partial half-life of $(3.2 \pm 0.3) \times 10^4$ y.

The fraction of ^{248}Cf alpha decays proceeding to excited levels in ^{244}Cm was measured by determining the fraction of alpha particles in coincidence with L X-rays arising from internal conversion decay of the excited levels in curium. This fraction, 0.170 ± 0.005, results in a calculated hindrance factor of ≥ 3.1 for decay to the first excited level in ^{244}Cm at 42.9 keV.

---

* National Bureau of Standards, Washington, D.C.
** USNDC Report, dated 10 October 1972, UCID-16136.

6. Transmission Data Analysis for Neutrons on ^{207}Pb (T. W. Phillips and B. L. Berman)

Data from the two-parameter measurement of the neutron total cross section of ^{207}Pb obtained as described in a previous report* is being analyzed to yield information on the decay width, spin, and parity of the levels of ^{208}Pb. The transmission function for neutrons has been obtained for energies between 90 and 1000 keV. The analysis of this transmission function is complicated by interference effects between adjacent levels and interference with the appreciable potential scattering which occurs at these energies. It has been found that to adequately account for these effects a large number of levels must be fit simultaneously. A computer code is being acquired to handle this problem. In the interim, a code which handles up to three levels with two possible spin states has been used. An example of the fit obtained in this manner is shown in Fig. A-1. The parameters for the three levels used in this fit are listed below.

E-resonance (keV)	Width (keV)	Spin and Parity
317.5	0.850	1^-
317.7	4.0	1^+
330.0	8.5	1^-

7. The ^{128}Te (n,γ) and ^{130}Te (n,γ) Cross Sections from 0.5 eV to 7 keV and the Xenon Anomaly in Old Tellurium Ores (J. C. Browne and B. L. Berman)

Preliminary results of this experiment were presented in a previous USNDC report.** Analysis of these data has been completed. Figures A-2 and A-3 show the ^{128}Te (n,γ) and ^{130}Te (n,γ) cross sections along with data taken using a natural tellurium sample. No resonances were observed for ^{128}Te below 425 eV and for ^{130}Te below 1143 eV. Calculation of the resonance absorption integral for the 16 resonances assigned to ^{128}Te and for the 6 resonances assigned to ^{130}Te indicates that the ratio of $^{129}Xe/^{131}Xe$ that could be formed in tellurium ores which were bombarded by a 1/E neutron flux is 3.8 ± 0.55. The measured ratio† in tellurium ores varies from 1.6 to 3.0. The ratio of $^{129}Xe/^{131}Xe$ predicted by thermal-neutron capture alone is 0.6. Therefore, the measured ratio will depend on the thermal/epithermal flux ratio incident on the tellurium ores throughout their history.

---

* T. W. Phillips and B. L. Berman, USNDC Report dated 10 November 1971, UCID-15937.

** J. C. Browne and B. L. Berman, USNDC Report dated 10 October 1972, UCID-16136

† B. Srinivasan, E. C. Alexander, Jr. and O. K. Manuel, J. Inorg. Chem. 34, 2381 (1972).

Previous neutron total cross-section measurements* on natural tellurium have extracted $ag\Gamma_n^o$ for various resonances in this energy range. (a = fractional abundance of an isotope). Since we can assign resonances to ^{128}Te and ^{130}Te, we can thus obtain values of $g\Gamma_n^o$ for these resonances. These values of $g\Gamma_n^o$ are listed in Tables A-1 and A-2 From the area under these resonances we can also extract values for $g\Gamma_\gamma$ for these resonances which are listed in Tables A-1 and A-2.

Table A-1. ^{128}Te Resonance Parameters

Present Results		Previous Measurements	
E_o	$g\Gamma_n\Gamma_\gamma/\Gamma$ (meV)	$g\Gamma_n^o$ (meV)*	$g\Gamma_\gamma$ (meV)
424.9	14.4	1.20	34
436.4	9.2	0.5	74
944	8.8	0.17	--
1323	5.85	0.09	--
1461	23.7	2.83	39
1587	6.2	0.25	17
1839	26.7	12.3	28
2969	21.2	14.5	22
3268	47.4	1.42	114
3549	27.9	0.5	398
4082	30.1	0.79	75
4256	10.45	0.38	18

Table A-2. ^{130}Te Resonance Parameters

Present Results		Previous Measurements	
E_o	$g\Gamma_n\Gamma_\gamma$ Γ (meV)	$g\Gamma_n^o$ (meV)*	$g\Gamma_\gamma$ (meV)
1143	7.85	0.32	29
1715	21.5	1.02	44
3201	25.9	0.84	57
4450	31.7	2.0	42

* S. Wynchank, J. B. Garg, W. W. Havens, Jr. and J. Rainwater, Phys. Rev. 166, 1234 (1968).

8. Capture γ-Ray Spectra for ^{181}Ta (n,γ) from 2 eV to 5000 eV. (M. L. Stelts and J. C. Browne)

The spectra of γ-rays from the ^{181}Ta (n,γ) reaction have been measured for incident neutrons in the energy range of 2 eV to 5000 eV using the LLL linac. The γ-rays from the Ta sample located at 13.4 meters from the neutron source were detected by a three-crystal (Ge(Li) - NaI) spectrometer with an energy resolution of 6 keV for 6-MeV photons. The energy scale and absolute efficiency were measured using calibrated radioactive sources and the Cl $(n_{thermal},\gamma)$ reaction. Data were stored on a magnetic drum in a two-dimensional array of 4096 pulse-height channels by 624 time-of-flight channels. The resolution of the experiment was such that most resonances below 200 eV were resolved.

Figure A-4 shows a portion of the pulse-height spectrum for the highest energy γ-rays obtained by summing over all neutron energies from 2 eV to 60 eV. The ground-state transition is indicated by "GS" and higher excited states by integer labels. All levels seen in the ^{181}Ta (d,p) reaction* and the ^{181}Ta $(n_{thermal},\gamma)$ reaction** below 1-MeV excitation energy are seen here plus many states not excited in these reactions.

The γ-ray spectra for individual neutron resonances exhibit marked intensity variations from resonance to resonance for the various transitions. Data analysis to extract the partial γ-decay widths for individual resonances is in progress.

9. Capture Cross-Section Measurements (J. B. Czirr and M. L. Stelts)

A paper with the title Capture Cross-Section Measurements for ^{165}Ho and ^{197}Au has been submitted for publication. The abstract for this paper is as follows:

As part of a continuing program to accurately measure neutron-capture cross sections, we have obtained data for ^{165}Ho and ^{197}Au in the 167 eV to 0.6 MeV energy range.

All capture reactions are measured relative to the fission rate of ^{235}U for neutron energies above 800 eV and to the ^{10}B $(n,\alpha_0+\alpha_1)$ reaction below 20 keV. In addition, current best estimates of $\sigma_F(^{235}U)$

* J. R. Erskine and W. W. Buechner, Phys. Rev. 133, B370 (1964).

** G. A. Bartholomew, J. W. Knowles, G. Manning and P. J. Campion, Atomic Energy of Canada Limited. Progress Report No. 517 (1957), unpublished.

and $\sigma_{n,\alpha}(^{10}B)$ are used to convert these ratios to up-to-date capture cross sections. The 3.9 eV "black resonance" of ^{165}Ho is used to normalize all cross sections.

Data have also been obtained for natural In in the 300 eV to 0.6 MeV energy range and will be published in the near future.

10. Cross Sections for Gamma-Ray Production by 14-MeV Neutrons
(L. G. Multhauf and S. M. Matthews)

For many elements, γ-ray production cross sections at 14-MeV neutron energy either have not been accurately measured, or can not be determined with confidence due to inconsistencies in reported values. We are undertaking, therefore, to measure this cross section for a range of elements using the high-flux 14-MeV-neutron facility at LLL.

The samples are placed in a ring geometry about the neutron source at a distance of 8 meters from the detector which is shielded from the major sources of neutron-induced background by a 1.9-meter-thick cement wall. In addition, time-of-flight measurements provide a clean separation between γ-rays produced in the sample and scattered neutrons. Preliminary measurements have shown background levels to be very low.

Monte Carlo calculations are being made for each sample material to determine the effects of both γ scattering and neutron multiple scattering. Ring dimensions for each element will be chosen such that these effects are either negligible or small enough that a correction can be made to the spectrum.

The detector systems consist of a 30-cm x 30-cm NaI(Tℓ) annulus operating in an anticompton mode, and having as a central detector either a large volume (Ge(Li) crystal or a NaI(Tℓ) well crystal of dimensions selected to optimize the peak efficiency and peak-to-total ratio. The well detector will be used to measure continuum γ-rays. The measured spectra will then be unfolded using measured detector response functions.

We have constructed a set of proton-recoil counters to measure the neutron flux. We will also use isotopic activation for an independent determination of the flux. We have employed, for example, ^{24}Na activation, using the well measured ^{27}Al(n,σ) cross section.

B. PHOTONUCLEAR PHYSICS

1. Photoneutron Cross Sections of ^{55}Mn and ^{59}Co (R. A. Alvarez, B. L. Berman, F. H. Lewis, and P. Meyer)

We have measured the photoneutron cross sections of ^{55}Mn and ^{59}Co from threshold to 36 MeV using photons from in-flight annihilation of positrons from the new Livermore positron-electron linac. The technique and apparatus used were essentially identical to those employed in a number of previous experiments; a description appears in the literature.* The principal differences in the present measurement were the higher available positron beam currents (which made possible measurements with higher photon energy resolution) than were available on the old Livermore linac, and a remote-controlled target-sample changer, which allowed measurements at each beam energy to be made on each isotope with identical accelerator and beam-transport system tuning. This improvement in the technique provides added confidence that fine structure observed in one isotope but not the other is indeed an effect of the nuclear dynamics and not a fluctuation caused by the apparatus.

Our results are shown in Figs. B-1 and B-2. The photon energy resolution is approximately 90 keV at 10 MeV and 160 keV at 35 MeV. Error bars shown are statistical only. In addition there are several sources of systematic uncertainty, which could introduce overall errors into the absolute cross section of up to about 10% in the region of the giant resonance peak and perhaps 40% at 35 MeV.

In both nuclei the giant resonance is rather broad and is divided into three main groups of substructures. There is a considerable amount of superimposed fine structure from theshold to 25 MeV or higher. Fine structure is evident in the $(\gamma,2n)$ cross section of both isotopes, as well. The integrated total cross sections are 807 MeV-mb for ^{55}Mn and 894 MeV-mb for ^{59}Co, while the integrated $(\gamma,2n)$ cross sections are 166 MeV-mb and 139 MeV-mb, respectively. The $(\gamma,3n)$ cross sections of both nuclei are very small.

C. APPLICATIONS

1. Intense Sources of Fast Neutrons (H. H. Barschall)

Methods for producing intense sources of neutrons of average energy above 10 MeV are investigated for applications in biology, medicine, radiation damage studies particularly for the CTR program, and cross section measurements.

---

* B. L. Berman *et al.*, Phys. Rev. 162, 1098 (1967).

(a) Intense source of 15-MeV D-T neutrons. The rotating tritium target previously described has been replaced by a 22-cm diameter target. (UCRL-74285). The new target permits operation at higher source strength. In 30 hours of operation at a source strength between 2.5 and 3.0×10^{12}/sec no appreciable decrease in source strength was observed. During this operation a fluence of $10^{17}/cm^2$ was delivered to a small sample for radiation damage studies. A new high-voltage power supply, which is scheduled for delivery in June 1973, should permit operation at higher source strength.

(b) A study of the neutron production from deuteron bombardment of deuterium, lithium, beryllium, and carbon targets has been completed. In UCRL 51310-Addendum, spectra and yields are given for the following conditions:

Target	Deuteron Energy (MeV)	Lab Angle
Thick Li	5 - 19	3^o - 32^o
Thick Be	3 - 20	3^o - 32^o
Thick C	12 - 18	3^o - 32^o
Thin D	16.5 and 18.6	3^o, 9^o, 32^o
Thin Be	5 - 18	3^o - 32^o

Average neutron energies and available doses are presented in UCRL-51310.

2. Ozone-Tagging for Biomedical Purposes (P. Meyer)

Ozone has been identified as a significant component of ambient air pollution where atmospheric photochemical activity occurs. The importance of ozone (O_3) as a toxicant is recognized and several of its effects have been defined, although the damage mechanism is still uncertain. At present, the distribution of the ozone-uptake throughout the respiratory system is unknown.

We have investigated the possibility of tagging ozone with an oxygen isotope, ^{15}O, a positron emitter with a half life of 122 seconds. With the use of the Anger positron camera* at the Livermore Linac, one can then in principle visualize the distribution of the radioactive ozone (or other gases) by observing the annihilation gamma rays from the decaying oxygen isotope.

The ^{15}O isotope is obtained by irradiating ^{16}O, with bremsstrahlung from the 100 MeV Linac, via a (γ,n) reaction in ^{16}O. The measurement of the ratio of activated to unactivated ozone, $O_3{}^*/O_3$, is the object of this experiment. Results using O_2 as a target gas indicate that an O_3 concentration of 1 ppm and a ratio of $^*O_3/O_3$ of 8×10^{-10} are the saturation points at the end of an irradiation. All the ozone is trapped at dry-ice temperature and then mixed with a breathing gas in varying proportions for use in a practical application.

*H. O. Anger, Scintillation Camera and Positron Camera in Medical Radioisotope Harming, (IAEA, Vienna, (1959), p. 59.

Preliminary experiments with small dogs have recently been carried out with the 16-inch diameter Anger camera at Livermore. Ozone concentrations used were 1 ppm and 5 ppm. Early results indicate that oxygen as a target gas provides sufficient amounts of tagged ozone to do useful lung function studies with ozone concentrations of perhaps $\geq$ .1 ppm. Activated nitrogen, ^{13}N, carbon dioxide, ^{11}C, and oxygen were also used for comparison. Data analysis is in progress at this time.

D. FACILITIES

1. Livermore Cyclograaff Facility (J. C. Davis and J. D. Anderson)

The Livermore Cyclograaff is the successor to the 90" variable energy cyclotron used for basic and programmatic research at Livermore for fifteen years. The 90" cyclotron was shut down and dismantled in February 1971 and the cyclograaff became fully operational for experimental use in late 1972. Easy production of high resolution or pulsed proton beams over the 1-27 MeV energy range was the primary advantage of the cyclograaff as a replacement accelerator. However, the high versatility with respect to particle species, beam energy, and beam intensity as well as significant financial advantages over alternate accelerators were important in the selection of the cyclograaff. The physical layout of the cyclograaff facility is shown in Fig. D-1. Most of the nuclear physics experiments in progress utilize microampere proton beams in either a high resolution mode for charged particle spectroscopy ($\Delta E/E \leq 0.1\%$) or in a pulsed mode for neutron time-of-flight and gamma ray production studies ($\Delta t \sim 1$ ns, $f \sim 5$ MHz). Similar work will be done with the 1-20 MeV deuteron beam. A detailed description of the accelerator facility and the pulsed beam capbilities appears in the June 1973 issue of the IEEE *Transactions On Nuclear Science.*

Figure A-1

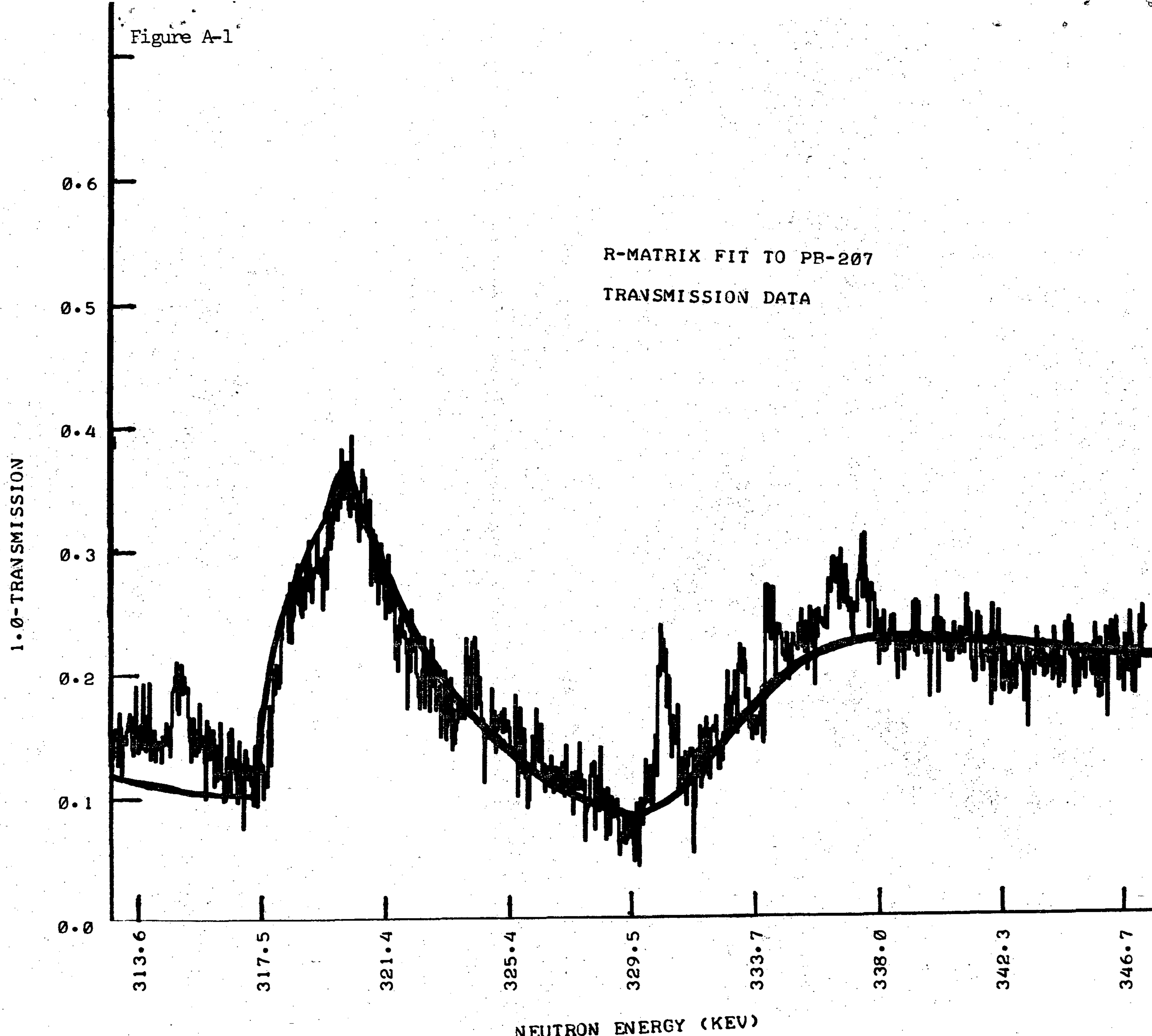
R-MATRIX FIT TO PB-207
TRANSMISSION DATA
1.0-TRANSMISSION
0.6
0.5
0.4
0.3
0.2
0.1
0.0
313.6
317.5
321.4
325.4
329.5
333.7
338.0
342.3
346.7
NEUTRON ENERGY (KEV)

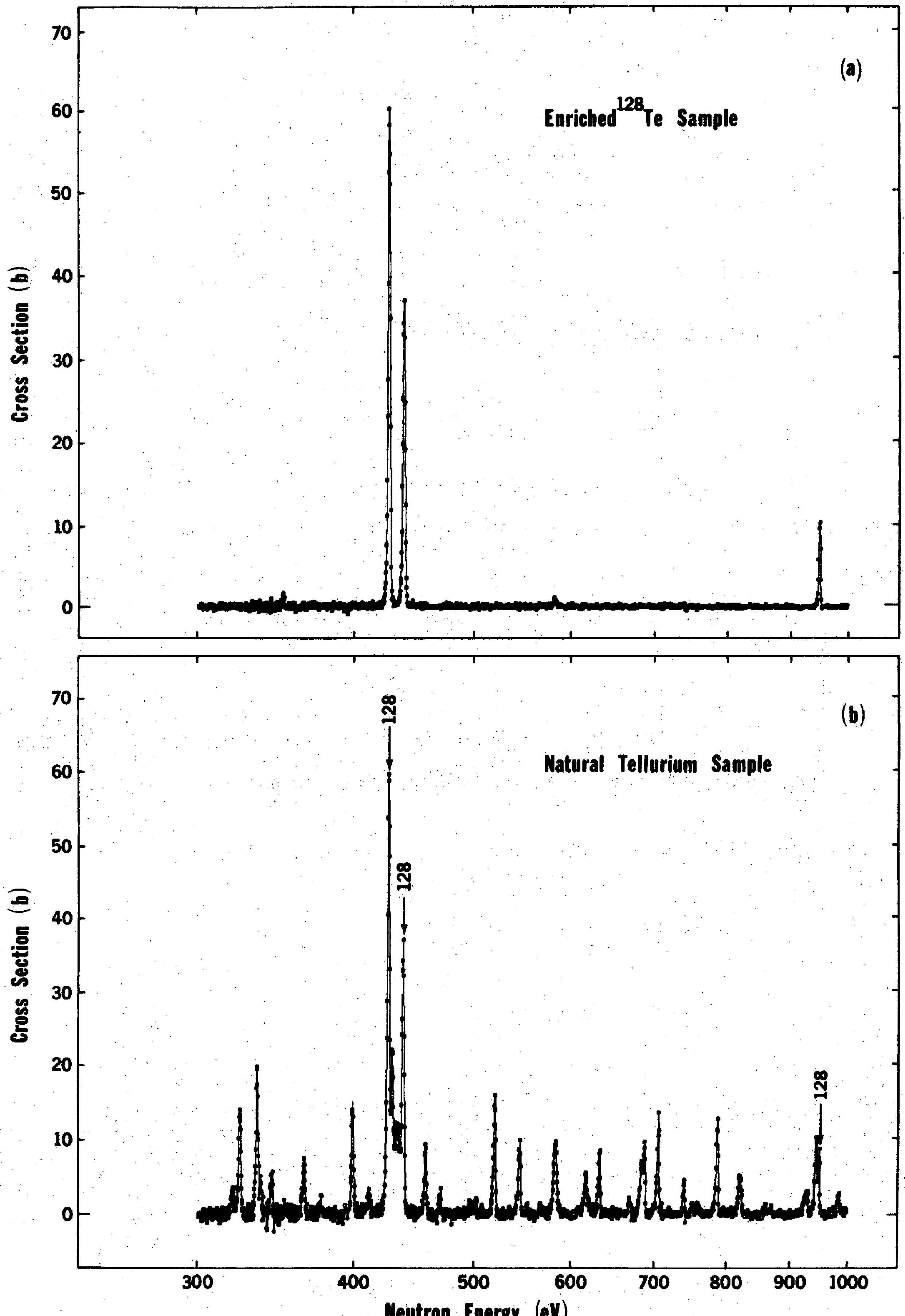

Figure A-2. The $^{128}Te(n,\gamma)$ Cross Section from 300-1000 eV. Ordinate scale for natural Te sample refers to ^{128}Te only.

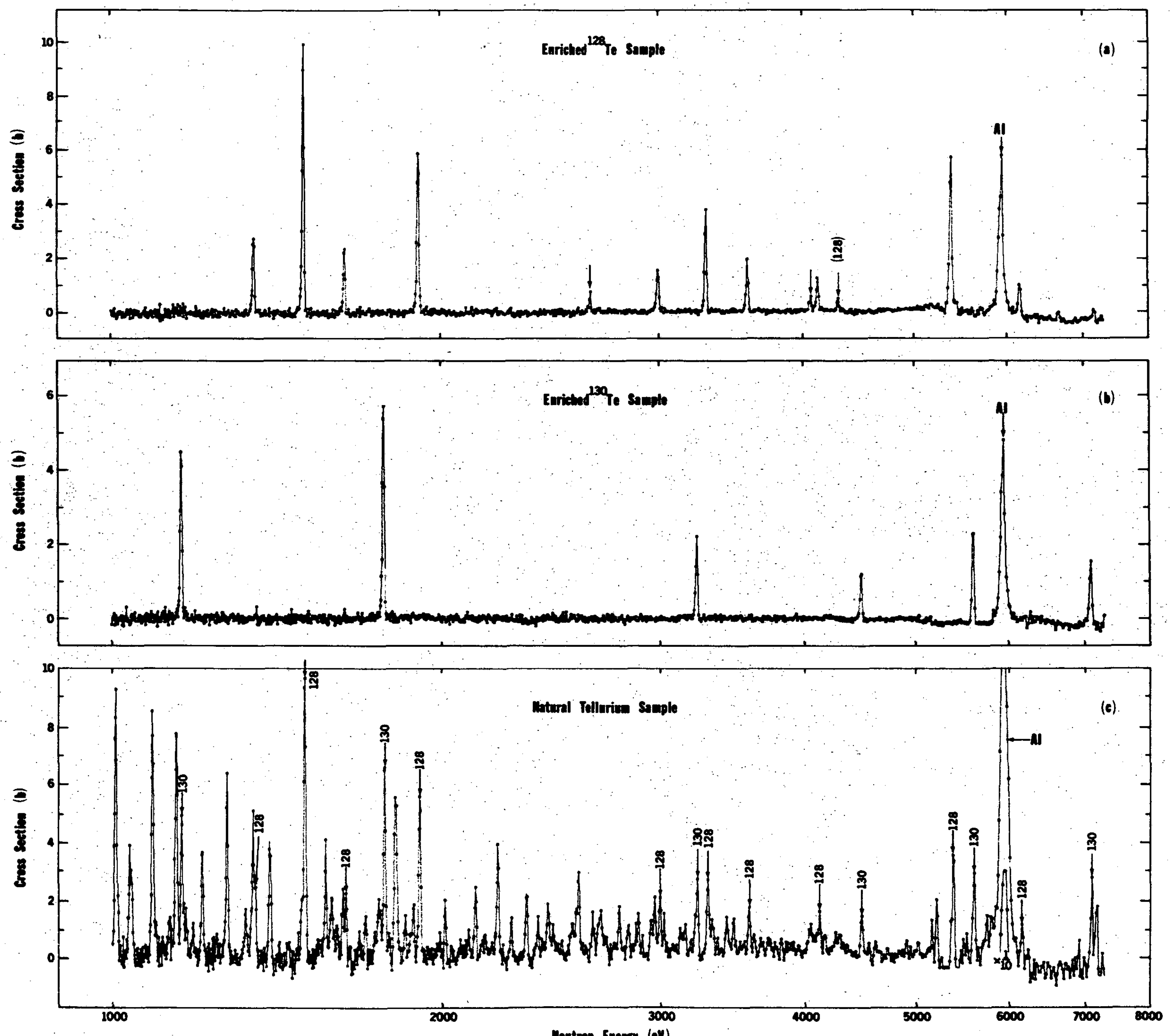

Figure A-3. The ^{128}Te (n,γ) and ^{130}Te (n,γ) Cross Sections from 1-7 keV. Ordinate Scale for natural Te sample refers to ^{128}Te and ^{130}Te resonances only.

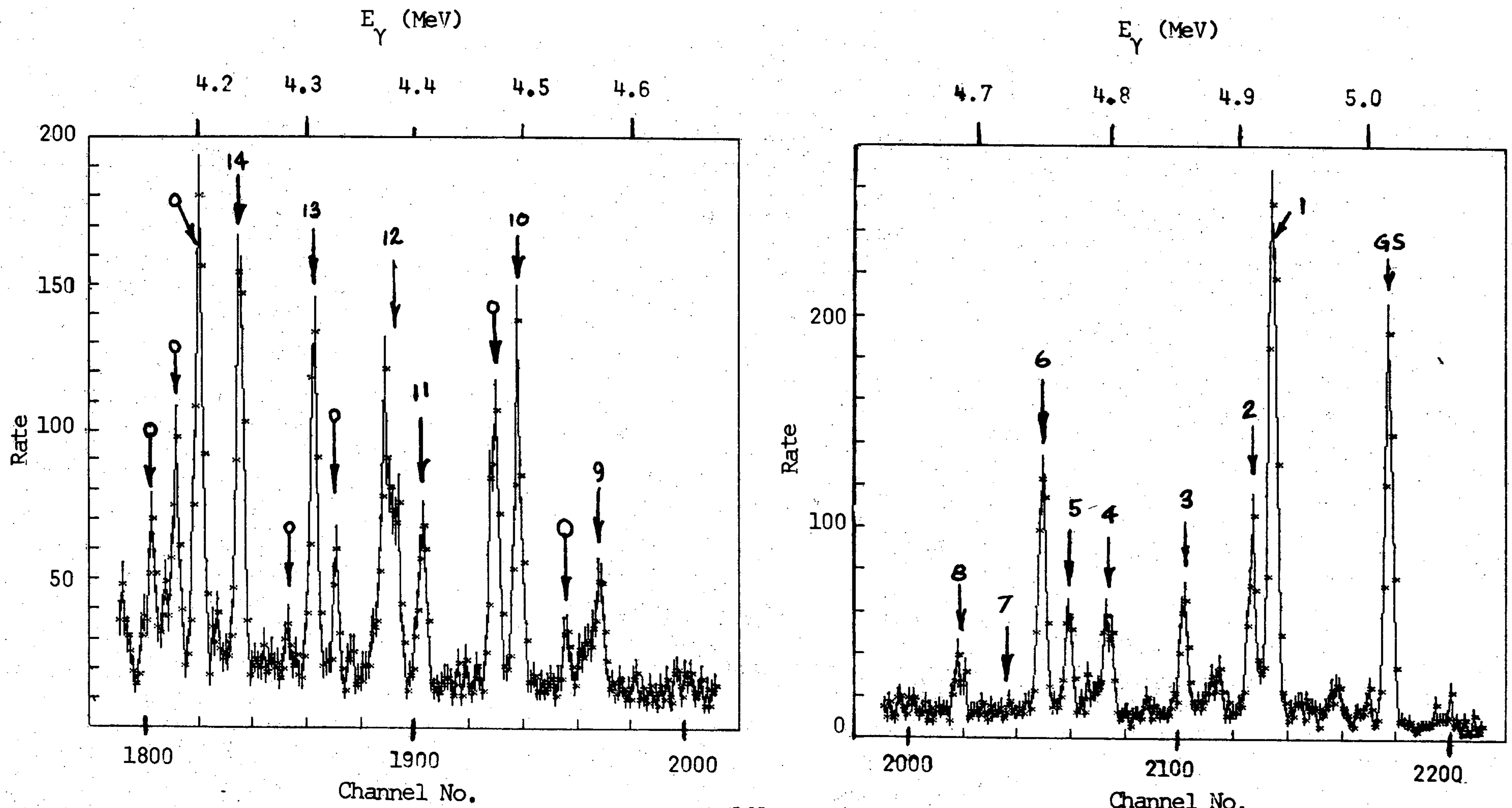

Figure A-4. A portion of the γ-ray spectrum from ^{181}Ta (n,γ) reaction for 2eV $\leq E_n \leq$ 60eV. The γ-ray energies refer to the double-escape peak as measured by the GeLi-NaI three-crystal spectrometer. The numbers listed on the peaks coincide with the levels seen in the ^{181}Ta (d,p) reaction. The peaks shown with an open circle were not observed in the (d,p) study.

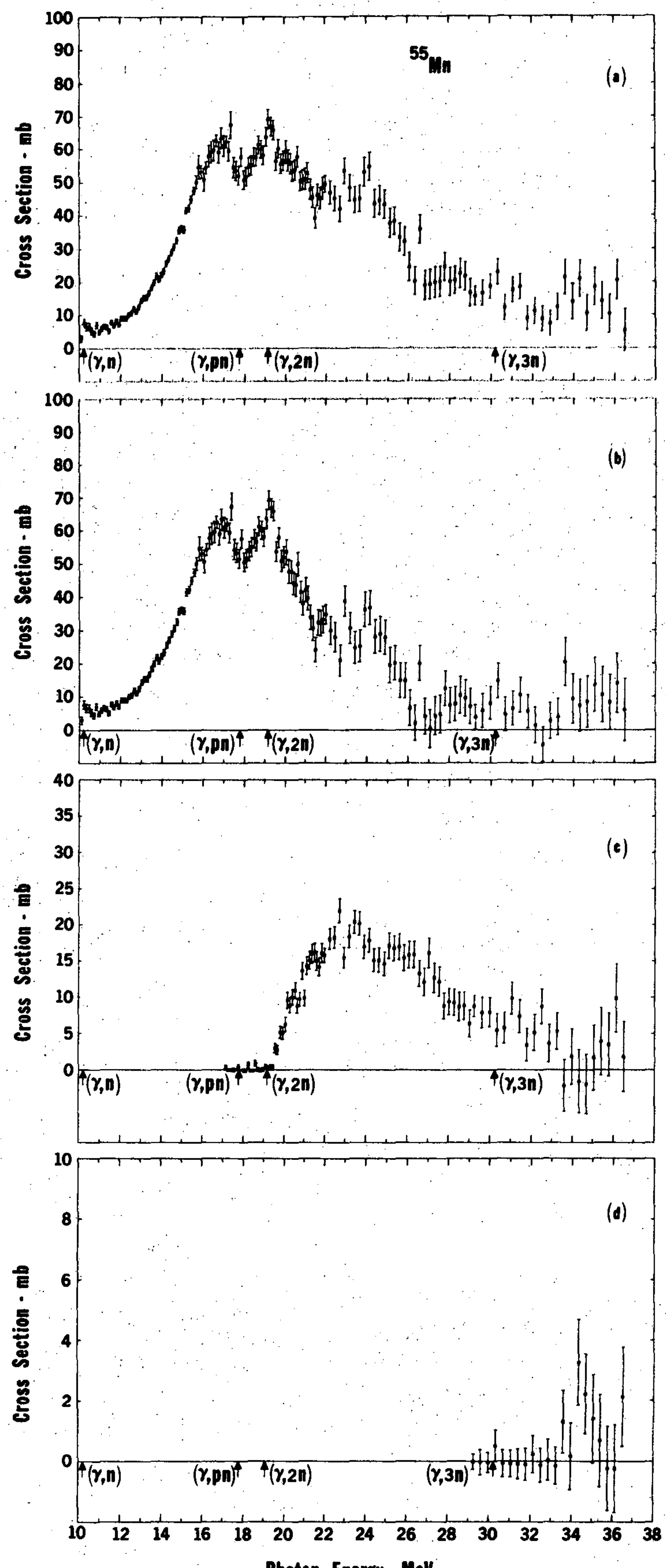

Figure B-1 Photoneutron cross sections of ^{55}Mn. Thresholds are indicated by arrows. (a) Total photoneutron cross section: $\sigma[(\gamma,n) + (\gamma,pn) + (\gamma,2n) + (\gamma,3n)]$; (b) $\sigma[(\gamma,n) + (\gamma,pn)]$; (c) $\sigma(\gamma,2n)$; (d) $\sigma(\gamma,3n)$.

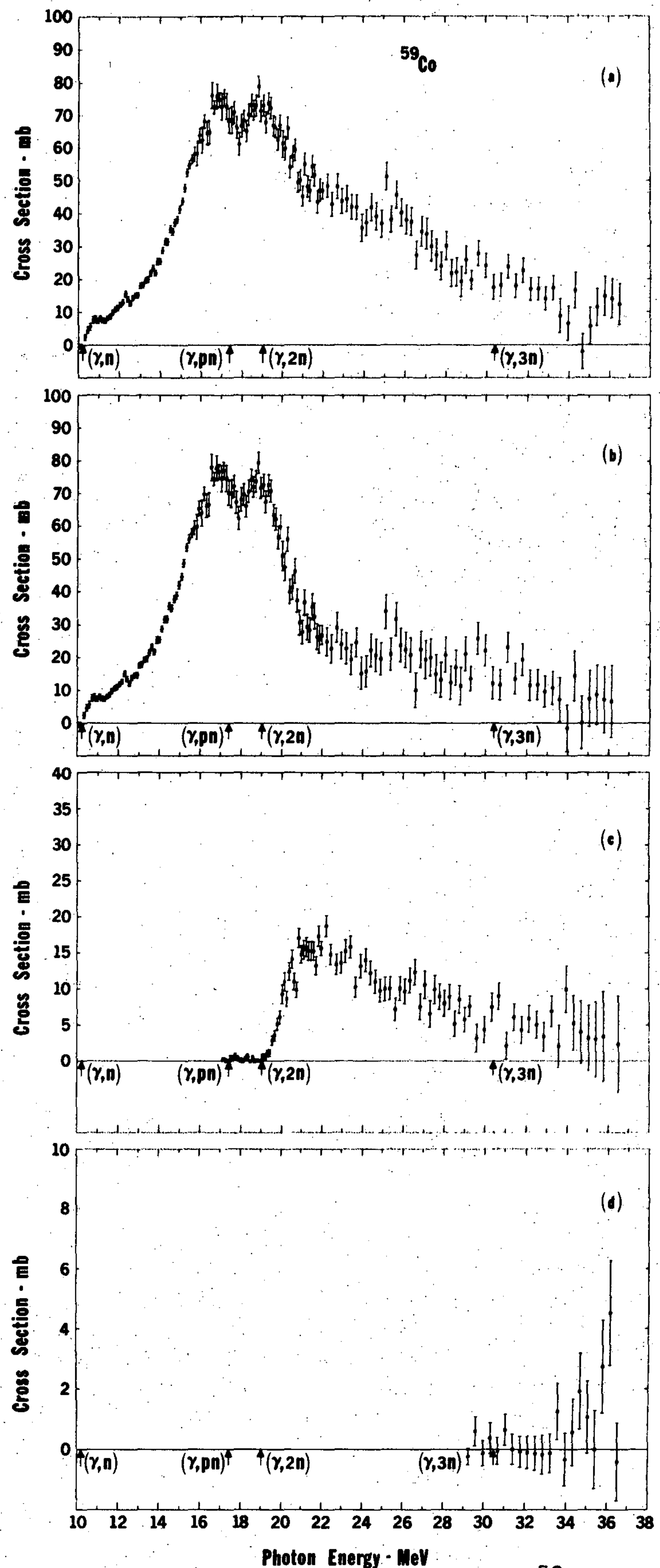

Figure B-2. Photoneutron cross sections of ^{59}Co. Thresholds are indicated by arrows. (a) Total photoneutron cross section: σ[(γ,n) + (γ,pn) + (γ,2n) + (γ,3n)]; (b) σ[(γ,n) + (γ,pn)]; (c) σ(γ,2n); (d) σ(γ,3n).

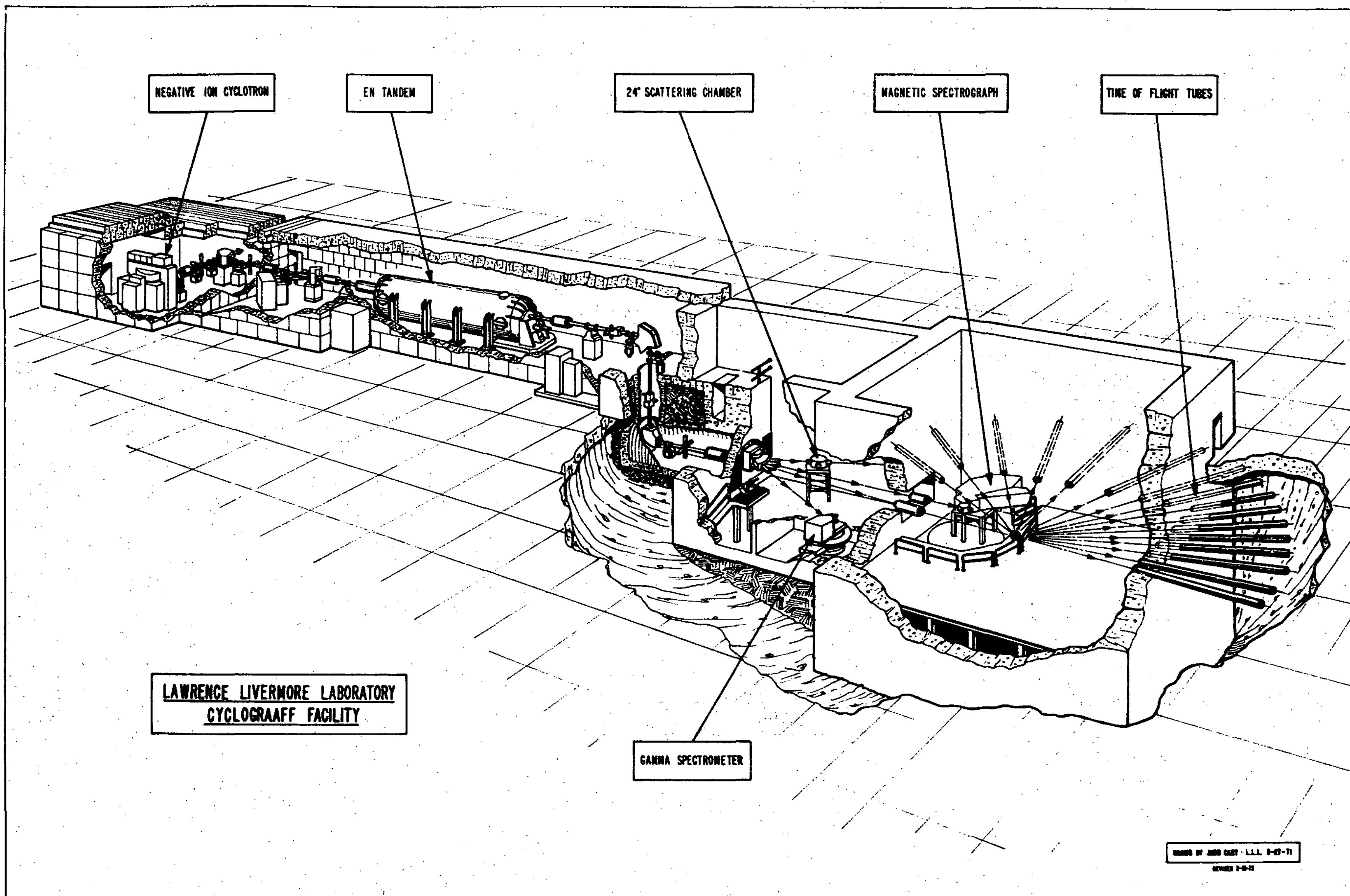
NEGATIVE ION CYCLOTRON
EN TANDEM
24" SCATTERING CHAMBER
MAGNETIC SPECTROGRAPH
TIME OF FLIGHT TUBES
LAWRENCE LIVERMORE LABORATORY
CYCLOGRAAFF FACILITY
GAMMA SPECTROMETER

Figure D-1

DISTRIBUTION

LLL Internal Distribution

R. E. Batzel	
E. Teller	
N. Keeler	
J. Anderson	10
H. Barschall	
B. Berman	
J. Browne	5
J. Czirr	
J. Davis	
E. Hulet	
F. Lewis	
R. Lougheed	
S. Matthews	
P. Meyer	
L. Multhauf	
T. Phillips	
R. Ragaini	
G. Sidhu	
M. Stelts	
J. Wild	
B. Pereira	
TID Berkeley	
TID File	5

External Distribution

Dr. Harry Alter
Atomic International
P.O. Box 309
Canoga Park, Ca. 91305

External Distribution (Continued)

Mr. William Bartels
Div. of Nuclear Materials
Security (MR-1303)
U. S. Atomic Energy Commission
Washington, D. C. 20545

Professor R. C. Block
Department of Nuclear Engineering
and Science
Rensselaer Polytechnic Institute
Troy, New York 12181

Dr. C. D. Bowman
Dr. R. S. Caswell
National Bureau of Standards
U. S. Department of Commerce
Washington, D. C. 20234

Dr. R. M. Brugger
Idaho Nuclear Corporation
P.O. Box 1845
Idaho Falls, Idaho 83401

Dr. V. J. Orphan
Gulf Radiation Technology
P.O. Box 608
San Diego, Ca. 92112

Dr. L. F. Chase, Jr.
Dr. H. A. Grench
Lockheed Palo Alto Research Lab.
3251 Hanover Street
Palo Alto, California 94304

Dr. Robert E. Chrien
Physics Department
Brookhaven National Laboratory
Upton, New York 11973

Dr. D. Eccleshall
Deputy Chief, Nuclear Effects Lab.
U.S. Army Ballistic Research Labs.
Aberdeen Proving Ground, Md. 21005

External Distribution (Continued)

Professor Herbert Goldstein
Rm. 242, S. W. Mudd Building
Columbia University
New York, New York 10027

Professor W. W. Havens, Jr.
Department of Physics
Columbia University
New York, New York 10027

Mr. Philip B. Hemmig
Div. of Reactor Development
and Technology
U. S. Atomic Energy Commission
Washington, D. C. 20545

Dr. Daniel J. Horen
Dr. F. G. J. Perey
Dr. Donald Steiner
Oak Ridge National Laboratory
P.O. Box X
Oak Ridge, Tennessee 37831

Dr. Harold E. Jackson
Dr. Alan B. Smith
Argonne National Laboratory
9700 South Cass Avenue
Argonne, Illinois 60439

Professor M. H. Kalos
Courant Inst. of Math. Science
New York University
251 Mercer Street
New York, New York 10012

Dr. George A. Kolstad, Asst. Dir.
Physics & Mathematics Programs
Div. of Research
U. S. Atomic Energy Commission
Washington, D. C. 20545

Professor Raymond Lane
Department of Physics
Ohio University
Athens, Ohio 45701

External Distribution (Continued)

Dr. David R. Lide, Jr.
Office of Reference Data
National Bureau of Standards
Washington, D. C. 20234

Professor David Lind
Department of Physics
University of Colorado
Boulder, Colorado 94305

Dr. M. S. Moore
Dr. Richard F. Taschek
Los Alamos Scientific Laboratory
P.O. Box 1663
Los Alamos, New Mexico 87544

Professor H. W. Newson
Department of Physics
Duke University
Durham, North Carolina 27706

Professor Gerald C. Phillips
Department of Physics
Rice University
Houston, Texas 77001

Dr. James S. Robertson
Medical Physics Division
Brookhaven National Laboratory
Upton, New York 11973

Dr. W. S. Rodney
Physics Section
National Science Foundation
Washington, D. C. 20550

Dr. George L. Rogosa
Division of Physical Research
U. S. Atomic Energy Commission
Washington, D. C. 20545

Professor Howard L. Schultz
Yale University
Electron Accelerator Laboratory
New Haven, Connecticut 06520

External Distribution (Continued)

Professor Edward M. Smith
Department of Radiology & Medicine
University of Miami
Coral Gables, Florida 33124

Dr. A. Stolovy
Naval Research Laboratory
Washington, D. C. 20390

Dr. W. E. Tucker
Texas Nuclear Corporation
P.O. Box 9267
Austin, Texas 78756

Dr. R. W. Wood
Div. of Biomedical and Environmental Research
U. S. Atomic Energy Commission
Washington, D. C. 20545